# NUCLEAR STRUCTURE -- THEORY

# CORE POLARIZATION AND THE COULOMB CORRECTION FOR NUCLEAR SCATTERING

Sam M. Austin, B.A. Brown and J.S. Winfield

A number of phenomena affect the difference in the mean field felt by protons and neutrons interacting with the same nucleus. If the nucleus has N > Z, then the symmetry potential makes the field for protons deeper than that for neutrons, reflecting the $V_\tau$ part of the two body potential (or alternatively, showing that the interaction between unlike nucleons is more attractive than that between like nucleons). But even for N = Z nuclei, the interaction may be made different by: (i) core polarization, (ii) a change in the effective energy of the interacting proton because of the repulsion by the charged target, and (iii) the possibility of a charge symmetry breaking (CSB) component of the effective interaction.[1,2] It is important to understand these effects both because they are interesting in their own right, as in the case of any CSB potential, and because they enter into phenomenological evaluations of the mean symmetry potential. The symmetry potential affects many aspects of nuclear structure, for example the splitting of the isovector and isoscalar components of giant resonances.

Commonly the empirical optical model (OM) potentials are corrected for the effect of the proton slowing down in the Coulomb field of the target nucleus by assuming that the mean energy of the proton is reduced by the average Coulomb energy $E_c$ felt by the proton. If we take the real potential to have an energy dependence given approximately by

$$V_R(E) = V_R(E=0) - \alpha E,$$

the Coulomb correction $V_{cc} = \alpha E_c$. For $\alpha = 0.3$ and $E_c = 1.73Z/R_c$ this yields $V_{cc} = 0.4Z/A^{1/3}$ (Ref. 3). For N>Z nuclei, one then extracts the value of the OM symmetry potential by correcting the proton potential for $V_{cc}$ before comparing it with the neutron potential. Unfortunately, $V_{cc}$ is not small compared to the effects of the symmetry potential and it seems unwise to rely entirely on such a simple theoretical model for the correction. For this reason, several attempts have been made to extract $V_{cc}$ from comparisons of neutron and proton scattering on N=Z nuclei. Published results,[3] based on spherical OM analyses for $^{40}Ca$, $^{32}S$, $^{28}Si$ and $^{16}O$, are generally consistent with $V_{cc} = 0.4Z/A^{1/3}$, although with rather large uncertainties. However, two criticisms can be made of these analyses: (i) the coupling to excited states in the target was ignored; and (ii) a somewhat arbitrary choice of the Coulomb radius (typically $r_c$=1.2 fm) was made. Indeed, the inclusion of channel coupling in the OM searches leads to large changes, at least for $^{32}S$ and $^{28}Si$, and the use of Coulomb potentials which reproduce the experimentally determined charge radii of the targets leads to a smaller but systematic change.[2] One obtains results such as those of Fig. 1. The potentials for n and p scattering from $^{28}Si$ and $^{32}S$ are essentially the same, corresponding to $V_{cc} = 0$, and inconsistent with the simple model.

Since it seems clear that the coupled channels results should be more reliable and since the effects that led to $V_{cc} = 0.4Z/A^{1/3}$ are almost certainly present, other important effects must have been ignored. One of possible significance is core polarization. In the work described in Ref. 2, we corrected for this through the results of bound state Hartree-Fock calculations with the SGII interaction of Ref. 4. These calculations show that the potential for neutrons is stronger for the outer part of the nucleus and that for protons is stronger in the nuclear interior, but that the cancellation is imperfect, so the net potential is stronger

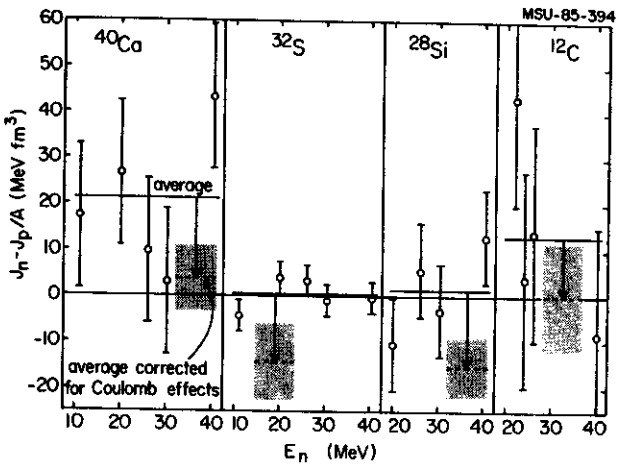


Fig. 1. Differences of volume integrals for neutron and proton scattering. The circles are the differences for the individual energies, the lines are the average differences for a given nucleus and the shaded regions give the values corrected by the Coulomb shift.

for neutrons. The core polarization correction will be larger for scattering states, since absorption will prevent the projectiles from fully sampling the nuclear interior (see below). To our knowledge no detailed estimate of the core polarization effect for scattering states has been made, but it appears that it might be 25% of the usual value of $V_{cc}$. Another unanswered question concerns the apparent difference of the results for the spherical nucleus $^{40}$Ca and for the deformed nuclei shown in Fig. 1. Were the core polarization correction larger for the deformed nuclei, this difference might be resolved.

Because of the importance of accurate estimates of the symmetry potential for structure phenomena and of limits on CSB, we have begun a study of these effects. A test of the effect of nuclear absorption on the core-polarization correction was made by adding the difference of the bound state Hartree-Fock potentials, $(V_p^{HF} - V_n^{HF})$ to a Woods-Saxon potential which describes neutron scattering from $^{40}$Ca at an energy E. The resulting potential was used to generate an angular distribution for proton scattering at energy $E+E_c$, and this is put into a standard OM search code to give the equivalent Woods-Saxon potential. The difference in the volume integrals of the initial and final Woods-Saxon potentials was found to be -6.4 MeV fm$^3$, compared to the direct difference $(V_p^{HF} - V_n^{HF})$ of -4.6 MeV fm$^3$. While this is clearly an improved estimate of the core-polarization correction, one is still starting from bound state potentials. As the volume integral corresponding to $0.4Z/A^{1/3}$ for $^{40}$Ca is about 20 MeV fm$^3$, these effects are substantial.

References.

1. NSCL annual report 1983-84, p. 92.
2. J.S. Winfield, S.M. Austin, R.P. DeVito, U.E.P. Berg, Z. Chen and W. Sterrenburg, Phys. Rev. C 33,1(1986); S.M. Austin, in Proc. Specialists Meeting on the Use of the Optical Model, Paris, Nov. 1985.
3. J. Rapaport, Phys. Rep. 87,25(1982); R.P. DeVito, S.M. Austin, U.E.P. Berg, R. De Leo and W.A. Sterrenburg, Phys. Rev. C28,2530 (1983).
4. N. van Giai and H. Sagawa, Phys. Lett. 106B,379(1981).

# FEEDBACK FROM PARTICLES INTO NUCLEI: DO WEAK-NEUTRAL CURRENTS PLAY A ROLE IN ANOMALOUS E1 TRANSITIONS?

Wm.C. McHarris and J.O. Rasmussen[a]

With the mounting evidence for parity-violating effects in atoms caused by interference of neutral-weak and electromagnetic currents,[1] one is tempted to look for similar effects in nuclei. The major difficulty is that neutral weak ("neutral-β") transitions would have to compete with γ transitions, which are intrinsically faster by factors in the vicinity of $10^9$. Parity-violating effects would be the most clear-cut signature; in addition, the first place to search would be where structure effects hinder γ transitions but perhaps not the competing β transitions.

The so-called anomalous E1 transitions in deformed heavy nuclei are good possibilities for scrutiny.[2] These transitions are often hindered by factors of $10^5$ or more, in at least one case by as much as $10^7$. In addition, the conversion coefficients for $s_{1/2}$ and $p_{1/2}$ electrons are anomalously large, at times by factors as high as several hundred. To a first approximation, the greater the degree of hindrance, the larger the anomalous conversion coefficient. In the past these have been explained, in a more or less ad hoc fashion by considering the penetration of the electrons into the nucleus and expanding the electronic wave-functions within the nuclear radius.[3] In large nuclei first-forbidden β transitions are increasingly enhanced, both because of the larger nuclear radii and because of the relativistic source-velocity terms, so that by the time the actinides are reached they are considerably faster than allowed transitions. A first-forbidden β transition would compete with an E1 γ transition, and for these particular "anomalous" E1's it is conceivable that much of the intrinsic difference in strength between weak and electromagnetic interactions has been accounted for. Specifically, "neutral-β decay" would masquerade to first order as the emission of conversion electrons -- there would be a nucleon-electron interaction at both the incoming and outgoing vertices of the diagrams, resulting in a type of electron scattering. Is it possible that a portion of the excess electrons attributed to these anomalous E1 transitions originates, in fact, from neutral-β decay?

The amplitude for low-energy neutral-weak coupling between an electron and a proton or neutron can be written respectively as[4]

$$M(e,p) = -(G_F/2\sqrt{2})\bar{u}_e'\gamma^\mu(1-4\sin^2\theta_W-\gamma_5)u_e \times \bar{u}_p'\gamma_\mu(1-4\sin^2\theta_W-1.25\gamma^5)u_p$$

and

$$M(e,n) = (G_F/2\sqrt{2})\bar{u}_e'\gamma^\mu(1-4\sin^2\theta_W-\gamma_5)u_e \times \bar{u}_n'\gamma_\mu(1-1.25\gamma^5)u_n$$

Thus, for the expected values of the Weinberg angle near 30°, neutrons, but not protons, contribute coherently to the amplitude, again enhancing the possible effect for very heavy nuclei.

We have been performing preliminary calculations and find it likely that neutral-β decay does contribute to the observed electron excess in some of these transitions. (This means that neutral-weak currents were, in effect, probably "observed" but not recognized as such some two decades ago.) Much remains to be done -- in particular, investigating the possible interference and parity-violating effects, such as recoil correlations.

a Lawrence Berkeley Laboratory

References

1. P. S. Drell and E. D. Commins, Phys. Rev. Lett. 53 (1984) 1984; see also the review article by E. N. Forston and L. L. Lewis, Physics Reports 113 (1984) 289.

2. F. T. Porter, I. Ahmad, M. S. Freedman, J. Milsted, and A. M. Friedman, Phys. Rev C 10 (1974) 803.

3. S. G. Nilsson and J. O. Rasmussen, Nucl. Phys. 5 (1958) 617.

4. E. D. Commins and P. H. Bucksbaum, Weak Interactions of Leptons and Quarks, Cambridge Univ. Press (1983), Chaps. 4 and 9.

# ISOSPIN-FORBIDDEN PROTON AND NEUTRON EMISSION IN 1s-0d SHELL NUCLEI

W.E. Ormand and B.A. Brown

One of the clearest indications of isospin mixing in light nuclei is the decay of T=3/2 states in A=4n+1 nuclei, by proton or neutron emission, to T=0 states in A=4n nuclei[1-3]. Previous studies[1-3] concluded that the spectroscopic amplitudes $\theta^{p(n)}_{INC}$ for these isospin-nonconserving (INC) transitions (1) systematically increase with mass A; (2) have an oscillation with period $\Delta A=8$ superimposed on the proton amplitudes; (3) are generally greater for neutron emission; (4) generally do not increase as a function of excitation energy. Perhaps the most striking of these features is the oscillation observed in $\theta^{p}_{INC}$. One cannot explain this periodicity in terms of simple schematic models[3], and thus it has been speculated[2] that this phenomenon is due to isospin mixing mediated by $\Delta$-isobars. In this report, results of detailed shell-model calculations of $\theta^{p(n)}_{INC}$ in the region $21 \leq A \leq 37$, where the full or nearly full 1s-0d (sd) major-shell configuration space is used, are presented. In our model, all the above features as well as the absolute magnitude of $\theta^{p(n)}_{INC}$ can be qualitatively understood. However, our results indicate that the variations from state to state is random or statistical in nature, rather than periodic.

In this work, we take into account INC effects due to admixtures of essentially all sd-shell T=1/2 states with the T=3/2 parent, and T=1 and 2 states with the T=0 daughter. Contributions due to the giant isovector monopole have been evaluated previously[4] using an harmonic-oscillator basis, and were found to be "small but not negligible"[5] compared to experiment. The harmonic-oscillator basis, however, tends to predict more isospin mixing in the ground state than does a more realistic Hartree-Fock calculation[5]. Therefore, we concentrate on the contributions due to mixing within the sd shell, and assume that the isovector monopole contribution is negligible.

Our calculations start with proton-neutron shell-model wave functions which have definite isospin. The model space consisted of A-16 nucleons outside an inert $^{16}$O core restricted to the $0d_{5/2}$, $1s_{1/2}$, and $0d_{3/2}$ orbits. The isoscalar Hamiltonian was taken to be the mass-dependent sd-shell Hamiltonian of Wildenthal[6].

Since the purpose of this investigation is to determine the influence of contributions due to mixing with individual parent and daughter states, a perturbation expansion for $\theta^{p(n)}_{INC}$ was used. In this formalism, $\theta^{p(n)}_{INC}$ is the sum of terms whose contribution is given by the product of the isospin-mixing amplitude and allowed spectroscopic amplitude. The isospin-nonconserving potential $V_{INC}$ was determined empirically by requiring that it reproduce experimental b- and c-coefficients of the isobaric mass multiplet equation (IMME; Mass = $a + bT_z + cT_z^2$) for sd-shell nuclei[7]. Details of the IMME calculation and the resulting $V_{INC}$ potential are given in Ref. 7.

From first-order perturbation theory, we see that it is quite possible that states which lie near the decaying T=3/2 state can contribute significantly to the total. Unfortunately, both the exact location and allowed spectroscopic amplitudes for these states are uncertain both theoretically and experimentally. To account for these uncertainties in the properties of the background T=1/2 states, the T=1/2 excitation energy spectrum was shifted relative to its original position by $\pm$ 500 keV in small steps of 10 keV. The "best" estimate of $\theta^{p(n)}_{INC}$ is then the average of the values obtained at each step. Upper and lower limits on the range of $\theta^{p(n)}_{INC}$ were then determined by evaluating both the upper and lower rms deviations away from this "best" value.

A comparison between experiment and our calculations is shown in Fig. 1 (experimental errors are typically less than 10% and have been

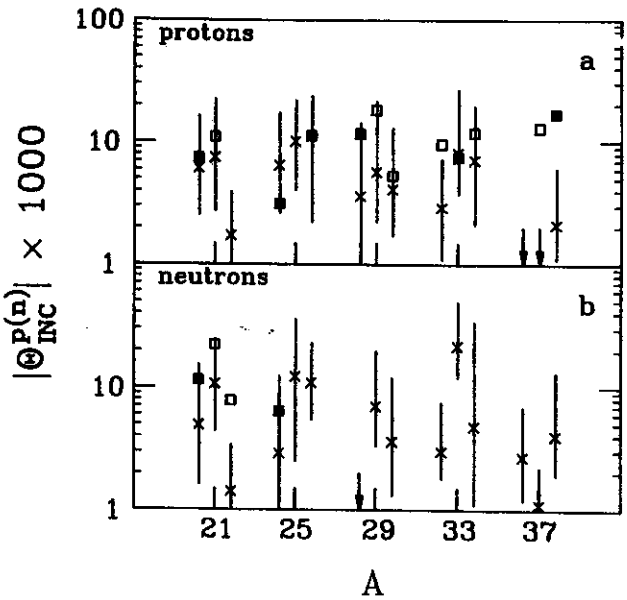


Fig. 1. Comparison between experimental and theoretical spectroscopic amplitudes for the isospin-forbidden decay of T=3/2 states by (a) proton and (b) neutron emission. For each A, one value of each spin is given and is plotted in the order: $2J^{\pi} = 5^+, 1^+, 3^+$. Experimental data are represented by squares (filled in for the lowest T=3/2 state for each A, and open for the remaining states). Crosses with error bars denote our "best" estimate and its upper and lower limits as described in the text.

suppressed from the figure). The error bars in the figure indicate the theoretical uncertainty due to the location of the background T=1/2 parent states. We find generally good agreement between experiment and our calculations, with the noted exception of A=37. However, in this region, the level density of sd-shell configurations is low compared to experiment, indicating that fp-shell configurations are important. Our results show that $\Theta^{p}_{INC}$ is roughly constant as a function of A, with fluctuations about this constant value. This is consistent with the known experimental data. The data for the lowest T=3/2 states in each nucleus show an oscillation with period $\Delta A=8$. However, the data for the remaining T=3/2 states fail to show this feature. Our results indicate that the observed variations in $\Theta^{p}_{INC}$ are due to random or statistical properties of the locations, the INC matrix elements, and the allowed spectroscopic factors of the nearby T=1/2 states.

Any difference between $\Theta^{p}_{INC}$ and $\Theta^{n}_{INC}$ which is not due to the different energy denominators used to evaluate the isospin-mixing amplitudes is attributable to the isotensor component of the INC interaction. This is because the isovector interaction can cause only $\Delta T=1$ mixing, and, therefore, would give equal isospin-mixing matrix elements in both the proton- and neutron-rich systems. The sd-shell experimental neutron amplitudes are 2 to 3 times greater than their proton counterparts. Our calculations do not show a systematic asymmetry between the proton and neutron amplitudes, although, individual cases may differ significantly.

The forbidden amplitudes for higher excited states have been evaluated, and were found to decrease slightly with excitation energy and to fluctuate in the same manner as the lower states. This is in agreement with experiment[3]. Although the density of background states is higher, and the isospin-mixing matrix elements are of the same order of magnitude as for lower states, we find that the decrease in $\Theta^{p(n)}_{INC}$ is due to a reduction in the magnitude of the allowed spectroscopic amplitudes.

At present, we are investigating the isospin-forbidden decay of T=5/2 and T=2 states in A=4n+1 and 4n nuclei, respectively.

References


1. R. Weigmann, R.L. Macklin and J.A. Harvey, Phys. Rev. C 14,1328(1976); F. Hinterberger, et al., Nucl. Phys. A352,93 (1981); F. Hinterberger, et al., Nucl. Phys. A424,200(1984); A.B. McDonald, J.R. Patterson, and H. Winkler, Nucl. Phys. A137,545(1969); J.C. Adloff et al., Phys. Rev. C 5,664(1972); P.G. Ikossi et al., Nucl. Phys. A274,1(1976).
2. J.F. Wilkerson, et al., Phys. Rev. Lett. 51,2269(1983).
3. A.B. McDonald and E.G. Adelberger, Phys. Rev. Lett. 40,1692(1978).
4. A. Lev and N. Auerbach, Nucl. Phys. A206, 563(1973).
5. N. Auerbach, Phys. Rep. 98,2731983).
6. B.H. Wildenthal, Progress in Particle and Nuclear Physics, ed. D.H. Wilkinson (Pergamon, Oxford, 1984) vol. 11, p.5.
7. W.E. Ormand and B.A. Brown, Nucl. Phys. A440,274(1985); the parameters used in this work are given in the first and seventh rows of Tables 2 and 3, respectively.

# ISOSPIN-MIXING CORRECTIONS TO FERMI β-DECAY

W.E. Ormand and B.A. Brown

In this report, corrections to the Fermi matrix element for superallowed β-transitions due to isospin impurities are presented. An important feature of these decays is that since they are purely vector, their ft values are given by

$$f_R t = \frac{K}{G_V^2 |M_F|^2}, \qquad (1)$$

where K is a constant, f the statistical rate function (which includes the nucleus-dependent "outer" radiative correction $\delta_R$ of Sirlin[1], i.e. $f_R = f(1 + \delta_R)$), t the partial half-life, $G_V$ the effective vector coupling constant for single nucleon β-decay, and $M_F$ the Fermi matrix element for the transition. Once all nucleus dependent corrections have been applied to Eq. (1), it is then possible to extract empirical values of $G_V$. This is important because the effective vector-coupling constants for nucleon and muon β-decay are related by

$$G_V^2 = G_\mu^2 \cos^2\theta_C (1 + \Delta_\beta - \Delta_\mu), \qquad (2)$$

where $\theta_C$ is the Cabibbo angle, and $\Delta_\beta$ and $\Delta_\mu$ are nucleus-independent "inner" radiative corrections to nucleon and muon β-decay, respectively. With $G_V/G_\mu$ and $\theta_C$ determined from experimental observations, it is then possible to test current theoretical estimates for $\Delta_\beta - \Delta_\mu$.

Although many superallowed transitions have been observed experimentally, at present ft values for only eight transitions have been measured with sufficient accuracy to permit a test of Eq. (1).[2] For this reason, this work concentrates on corrections for the ground state β-decay of $^{14}O$, $^{34}Cl$, $^{42}Sc$, $^{46}V$, $^{50}Mn$, and $^{54}Co$ and the decay of the metastable state in $^{26}Al$ and $^{38}K$.

If the initial and final nuclear states are perfect analogs, then the Fermi matrix element is model independent, and values for $G_V$ could then be extracted from measured ft values with Eq. (1). The most accurately determined ft values, however, are not constant within experimental uncertainty[2], suggesting the breaking of analog symmetry between the initial and final nuclei due to the presence of isospin nonconserving (INC) interactions.

The extent to which analog symmetry is broken is embodied in the correction factor $\delta_C$ to the Fermi matrix element, defined by $|M_F|^2 = |M_{F0}|^2 (1-\delta_C)$, where $M_{F0}$ is the Fermi matrix element between states with analog symmetry.

We have re-examined these corrections to the Fermi matrix element in the light of recent advances in our understanding of nuclear structure. Perhaps the most important improvements in regard to this problem are radial wave functions obtained from a self-consistent Hartree-Fock calculation utilizing a Skyrme-type interaction. In addition, revised isoscalar Hamiltonians and an INC interaction which reproduces experimental isotopic mass shifts have been used (see Ref. 3).

The starting point for our calculation of $\delta_C$ is the usual spherical shell-model wave functions, which possess definite isospin. Due to the wide range of nuclei under investigation, four separate shell-model configuration spaces were used in this work. These were: the 0p shell, the 1s-0d shell, the $0d_{3/2}$ and $0f_{7/2}$ orbits, and the 0f-1p shell (for more details, see Ref. 3). Within each basis it was necessary to consider the effects of isospin mixing between states within the model space as well as with those outside. Isospin mixing within the model space is calculated by adding the INC interaction onto the isospin-conserving Hamiltonian, while isospin mixing outside the sd shell is taken into account by allowing the proton radial wave functions to be pushed out relative to the neutron wave functions due to

the Coulomb potential. These two effects can be factored[4] into components due to the radial overlaps (RO) and isospin mixing within the configuration space (IM), $\delta_C = \delta_{RO} + \delta_{IM}$.

Previously[5], $\delta_{RO}$ was evaluated using proton and neutron radial wave functions obtained with a central Woods-Saxon (WS) plus Coulomb potential. This procedure overestimates the difference between the proton and neutron radial wave functions by neglecting an induced isovector interaction that arises from the difference between the proton and neutron densities. To take into account the effects of this induced interaction we have performed self-consistent Hartree-Fock (HF) calculations with a Skryme-type interaction (SGII, Ref. 6).

Values of $\delta_{RO}$ obtained with the Hartree-Fock wave functions are compared with those of Ref. 5 and are given in Table I. Values obtained with HF wave functions are systematically reduced relative to those given in Ref. 5. This reduction is due to the effects of both the Coulomb and nuclear central potentials used in each calculation. In Hartree-Fock calculations, we find that protons are effectively in a potential well which is both deeper at the origin and has a higher barrier at the nuclear surface relative to the WS procedure. This additional potential tends to draw in the proton radial wave functions relative to the neutrons, and, thus reduce the value of $\delta_{RO}$.

Table I

Comparison of the corrections to the Fermi matrix element obtained in the present work and with the values in Refs. 4 and 5. Values of $\delta$ are given in %.

| Decaying nucleus | Present Work | | | Previous Values[4,5] | | |
|---|---|---|---|---|---|---|
| | $\delta_{IM}$ | $\delta_{RO}$ | $\delta_C$ | $\delta_{IM}$ | $\delta_{RO}$ | $\delta_C$ |
| $^{14}O$ | 0.010 | 0.134 | 0.144 | 0.05 | 0.23 | 0.33 |
| $^{26m}Al$ | 0.012 | 0.255 | 0.267 | 0.07 | 0.27 | 0.34 |
| $^{34}Cl$ | 0.056 | 0.432 | 0.488 | 0.23 | 0.62 | 0.85 |
| $^{38m}K$ | 0.111 | 0.453 | 0.564 | 0.16 | 0.54 | 0.70 |
| $^{42}Sc$ | 0.109 | 0.209 | 0.318 | 0.13 | 0.35 | 0.48 |
| $^{46}V$ | 0.013 | 0.230 | 0.243 | 0.04 | 0.36 | 0.40 |
| $^{50}Mn$ | 0.004 | 0.296 | 0.300 | 0.03 | 0.40 | 0.43 |
| $^{54}Co$ | 0.005 | 0.359 | 0.364 | 0.04 | 0.56 | 0.60 |

a) values presented in Table 6 of Ref. 4

b) values presented in Table 3 of Ref. 5

The contribution $\delta_{IM}$ was evaluated with isospin-mixed wave functions obtained by adding the INC interaction onto the isoscalar Hamiltonian. The one-body transition density (OBTD) matrices for these wave functions were calculated, and $\delta_{IM}$ was determined by summing the product of the OBTD matrices and the single-particle matrix elements of the Fermi transition operator. $V_{INC}$ for each configuration space was determined empirically[3] by requiring that the parameters of a Coulomb plus phenomenological charge-asymmetric and charge-dependent potential reproduce experimental b- and c-coefficients of the isobaric mass multiplet equation

The isospin mixing corrections to the Fermi matrix elements are compared with those of Towner and Hardy[4], and are also listed in Table I. The values of $\delta_{IM}$ calculated here are much smaller than those of Towner and Hardy. This difference is due to both zeroth-order wave functions and the INC interaction used in each work.

A comparison between values of $G_V/G_\mu$ determined from experimental ft values and the results of the calculations presented here and those of Towner and Hardy are shown in Fig. 1 (the error bars reflect the limits of experimental precision). From the figure, it is clear that the extracted values of $G_V/G_\mu$ are not constant within experimental error. In fact, the results of Towner and Hardy give two inconsistent values: one for $Z < 21$, and another for $Z \geq 21$. The results reported here represent an improvement in this sense, as values of $G_V/G_\mu$ are consistent for Z=17, 21, and 25.

As was mentioned above, the uncertainties

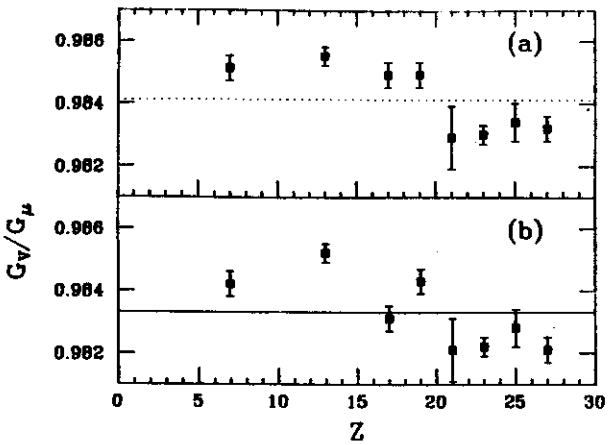


Fig. 1. Comparison between values of the ratio $G_V/G_\mu$ determined from experimental ft values and the $\mu$ corrections to the Fermi matrix element of (a) Towner and Hardy and (b) the present work. The line drawn in each figure represents the average value obtained in each work.

in $G_V/G_\mu$ examined thus far have been purely experimental. There are, however, some theoretical uncertainties as well. In particular, the effects of the model-space truncations on the 0p- and 0f-1p-shell nuclei are unknown. In the case of the 0p shell, no particle-hole excitations into the low-lying $0d_{5/2}$ and $1s_{1/2}$ orbits were allowed. As for the 0f-1p-shell nuclei, no more than one particle was allowed outside the $0f_{7/2}$ orbit. At present, there exists no isoscalar Hamiltonian for the nuclei in question which can adequately account for these effects. The situation concerning the 1s-0d-shell, however, is somewhat better. A full-space calculation for nuclei in the middle of the sd-shell is feasible within present limits of computing technology, and, recently, an improved isoscalar Hamiltonian that includes the full sd-shell has been developed[7]. With this in mind, perhaps the best experimental strategy for the future would be to concentrate on understanding the discrepancies that lie within the sd-shell. This course should also include more precise measurements of the ft values for the superallowed β-decays of $^{22}$Mg, $^{26}$Si, $^{30}$S, and $^{34}$Ar.

As an illustration of what can be learned from superallowed transitions, we conclude with some remarks regarding the nucleus-independent "inner" radiative correction $\Delta_\beta - \Delta_\mu$. The difference $\Delta_\beta - \Delta_\mu$ is given by[8]

$$\Delta_\beta - \Delta_\mu = \frac{\alpha}{2\pi}\left[\, 3\ell n(M_Z/M_p) + 6\bar{Q}(M_Z/M_A) + 2C + \ldots\right], \qquad (3)$$

where $M_Z$ is the Z-boson mass, $M_p$ the proton mass, $\alpha$ the fine-structure constant, and $\bar{Q}$ is the average quark charge (for u and d quarks $\bar{Q}$ is 1/6). The quantity C is the least understood part of Eq. (3), and present estimates are C = 1[9] and C= -0.5[10]. Using the values of $G_V/G_\mu$ obtained in the present work we find the quantity C to be 1.64(17) and -0.26(39) for the decay of $^{26m}$Al and $^{34}$Cl, respectively.

---

References


1. A. Sirlin, Phys. Rev. 164(1967)1767.
2. V.T. Koslowsky, Ph. D. Thesis, University of Toronto (1983)
3. W.E Ormand, Ph.D. thesis, Michigan State University (1985); W.E. Ormand and B.A. Brown, Nucl. Phys. A440(1985)274.
4. I.S. Towner and J.C. Hardy, Nucl. Phys. A205(1973)33.
5. I.S. Towner, J.C. Hardy, and M. Harvey, Nucl. Phys. A284(1977)269.
6. Nguyen Van Giai and H. Sagawa, Nucl. Phys. A371(1981)1.
7. B.H. Wildenthal, Progress in Particle and Nuclear Physics, edited by D.H. Wilkinson (Pergamon Press, Oxford, 1984) vol. 11, p.5.
8. A. Sirlin, Rev. Mod. Phys. 50(1978)573.
9. A. Sirlin, Nucl. Phys. B71(1974)29.
10. E.S Abers et al., Phys. Rev. 167(1968)1461.

# SHELL-MODEL CALCULATIONS FOR THE COEFFICIENTS OF THE ISOBARIC-MASS MULTIPLET EQUATION AND THE EMPIRICAL DETERMINATION OF ISOSPIN-NONCONSERVING POTENTIALS

W.E. Ormand and B.A. Brown

Wigner[1] was the first to demonstrate that the binding-energy (mass) differences between members of the same isobaric multiplet can be parameterized by

$$E(\nu,T_z) = a(\nu) + b(\nu)T_z + c(\nu)T_z^2, \qquad (1)$$

where the label $\nu$ represents all quantum numbers other the than the z-component of the isospin $T_z$. The coefficient $a(\nu)$ is due to both the isoscalar and isotensor components of the Hamiltonian, while $b(\nu)$ and $c(\nu)$ are due only to the isovector and isotensor parts, respectively. It is precisely these last two components that are responsible for the breaking of isospin symmetry, which has been the subject of recent study[2,3].

The exact form of the isovector and isotensor interactions are, at present, unknown, and it has been shown[4] that the Coulomb force alone cannot account for experimental isotopic mass shifts. With this in mind, empirical forms of the isovector and isotensor parts are proposed, and by performing a least-squares fit to experimental b- and c-coefficients the parameters of these interactions are obtained. With the isospin-nonconserving components of the Hamiltonian thus determined, it is then possible to make predictions as to the extent of isospin-symmetry violation in nuclei, and compare with experimental observations.

The starting point of the calculations of the b- and c-coefficients are shell-model wave functions obtained with an appropriate isoscalar Hamiltonian. Due to the wide range of nuclei ($14 \leq A \leq 54$) under investigation, four separate configuration spaces and isoscalar Hamiltonians were used. These are:

(1) $0p_{3/2}$ and $0p_{1/2}$ orbits (0p shell) and the interaction of Cohen and Kurath[5],

(2) $0d_{5/2}$, $1s_{1/2}$, and $0d_{3/2}$ orbits (1s-0d shell) and the mass-dependent sd-shell Hamiltonian of Wildenthal[6],

(3) $0d_{3/2}$ and $0f_{7/2}$ orbits and the isoscalar Hamiltonian of Hsieh and Wildenthal[7], and

(4) $0f_{7/2}$, $1p_{3/2}$, $0f_{5/2}$, and $1p_{1/2}$ orbits (0f-1p shell) and the van Hees interaction[8].

The isospin-nonconserving potential is assumed to have the form

$$V_{INC}^{(k)} = [C^{(k)}V_C(r) + P^{(k)}V_\pi(r) + R^{(k)}V_\rho(r) + A^{(k)}V_{Iso}]\, I^{(k)}, \qquad (2)$$

where $V_C(r)$ is the Coulomb potential $e^2/r$, $V_\pi(r)$ and $V_\rho(r)$ are Yukawa potentials of the form $V_\mu(r) = e^{-\mu r}/\mu r$, with $\mu_\pi = 0.7\text{fm}^{-1}$ and $\mu_\rho = 3.9\text{fm}^{-1}$, and $V_{Iso}$ represents the T=1 two-body matrix elements of the isoscalar Hamiltonian. The strength of each part of the interaction in Eq. (2) is embodied in the coefficients $C^{(k)}$, $P^{(k)}$, $R^{(k)}$, and $A^{(k)}$, which are assumed to depend only on the isospin tensor rank k (note, however, that the condition $C^{(1)}=C^{(2)}$ must be satisfied). $I^{(k)}$ is an isospin operator whose form permits the components $V_{INC}^{(k)}$ to correspond to the T=1 part of the proton-proton ($v^{(pp)}$), neutron-neutron ($v^{(nn)}$), and proton-neutron ($v^{(pn)}$) interactions (for more details see Ref. 3).

In this work, the two-body matrix elements of Eq. (2) were evaluated using harmonic-oscillator radial wave functions with an oscillator parameter appropriate for A=39, given by

$$\hbar\omega(A) = 45A^{-1/3} - 25A^{-2/3}\text{MeV}. \qquad (3)$$

Table I

Parameters for the "best" isovector interaction for each configuration shell-model space.

| $\varepsilon^{(1)}(p_{3/2})$ | $\varepsilon^{(1)}(p_{1/2})$ | $C^{(1)}$ | $P^{(1)}$ | $R^{(1)}$ | $A^{(1)}$ |
|---|---|---|---|---|---|
| 0p Shell | | | | | |
| 1.057(82) | 0.891(67) | 0.93(4) | 0.0 | 0.0 | -3.6(1) |

| $\varepsilon^{(1)}(d_{5/2})$ | $\varepsilon^{(1)}(s_{1/2})$ | $\varepsilon^{(1)}(d_{3/2})$ | $C^{(1)}$ | $P^{(1)}$ | $R^{(1)}$ | $A^{(1)}$ |
|---|---|---|---|---|---|---|
| 1s-0d Shell | | | | | | |
| 3.325(15) | 3.305(16) | 3.346(7) | 1.00 | 0.0 | 0.0 | 0.0 |

| $\varepsilon^{(1)}(d_{3/2})$ | $\varepsilon^{(1)}(f_{7/2})$ | $C^{(1)}$ | $P^{(1)}$ | $R^{(1)}$ | $A^{(1)}$ |
|---|---|---|---|---|---|
| $0d_{3/2}$ and $0f_{7/2}$ orbits | | | | | |
| 6.262(10) | 6.019(13) | 1.00 | 0.0 | 0.0 | 0.0 |

| $\varepsilon^{(1)}(f)$ | $\varepsilon^{(1)}(p)$ | $C^{(1)}$ | $P^{(1)}$ | $R^{(1)}$ | $A^{(1)}$ |
|---|---|---|---|---|---|
| 0f-1p Shell | | | | | |
| 7.460(10) | 7.200(84) | 1.00 | 0.0 | 0.0 | 0.0 |

The single-particle energies $\varepsilon^{(1)}(\rho)$ and the parameters $P^{(1)}$ and $R^{(1)}$ are given in MeV. The parameters $c^{(1)}$ and $A^{(1)}$ are dimensionless, with $A^{(1)}$ being given in units of $10^{-2}$. Note that the single-particle energies are appropriate for A=39, and must be scaled by the factor SF(A).

Since the matrix elements of the 1/r Coulomb and Yukawa-like potentials are proportional to $b_{osc}^{-1}$, where $b_{osc} = \sqrt{41.4/\hbar\omega}$ is the oscillator length parameter, the Coulomb and Yukawa INC matrix elements were multiplied by the scaling factor $SF(A) = b_{osc}(39)/b_{osc}(A)$. For most nuclei under consideration ($20 \leq A \leq 50$), the parameterization of $\hbar\omega$ given by Eq. (3) was sufficient. However, for other nuclei ($A < 20$ and $A > 50$) Eq. (3) is inadequate, and values of $\hbar\omega$ determined from experimental root mean square (rms) charge radii were used.

The data base for the least-squares fits were obtained from tabulations of ground-state binding[9] energies and excitation energies[10]. The resulting "best" parameters obtained from each least-squares fit to experimental b- and c-coefficients are presented in Tables I and II, respectively, with a comparison between experimental and theoretical values being shown

Table II

Parameters of the best isotensor interaction for each shell-model configuration space.

| Configuration space | $C^{(2)}$ | $P^{(2)}$ (MeV) | $R^{(2)}$ (MeV) | $A^{(2)}$ ($\times 10^{-2}$) |
|---|---|---|---|---|
| 0p Shell | 0.93(3) | 0.0 | 60(9) | 0.0 |
| 1s-0d Shell | 1.00 | 0.0 | 78(4) | 0.0 |

in Figs. 1-4 for b-coefficients and Figs. 5 and 6 for c-coefficients. The free parameters in the b-coefficient fits were taken to be the isovector single-particle energies $\varepsilon^{(1)}(\rho)$, for each valence orbit, the Coulomb strength parameter, and any one of the coefficients $P^{(1)}$, $R^{(1)}$, and $A^{(1)}$. For fits to c-coefficients the free parameters were taken to be the Coulomb strength and any one of the remaining isotensor strength coefficients. This restriction on the number of free parameters was imposed because the data were not sensitive to the determination of more than one parameter of the charge-asymmetric and charge-dependent interactions. In addition, fits to 0f-1p-shell b-coefficients were performed by requiring that $\varepsilon^{(1)}(0f_{7/2})=\varepsilon^{(1)}(0f_{5/2})=\varepsilon^{(1)}(f)$ and $\varepsilon^{(1)}(1p_{3/2})=\varepsilon^{(1)}(1p_{1/2})=\varepsilon^{(1)}(p)$. Fits to c-coefficients for nuclei in the $0d_{3/2}$-$0f_{7/2}$ orbits and the 0f-1p shell were not performed because there is very little experimental data in this region.

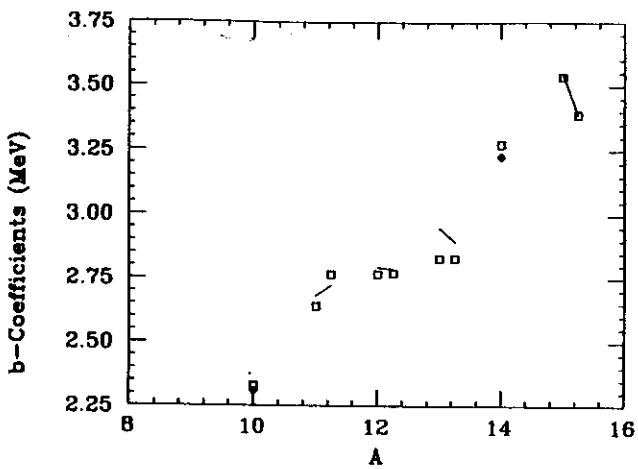


Fig. 1 Plot of 0p-shell b-coefficients. Experimental data are represented by open boxes, while the fitted values are given by the line and the solid diamonds.

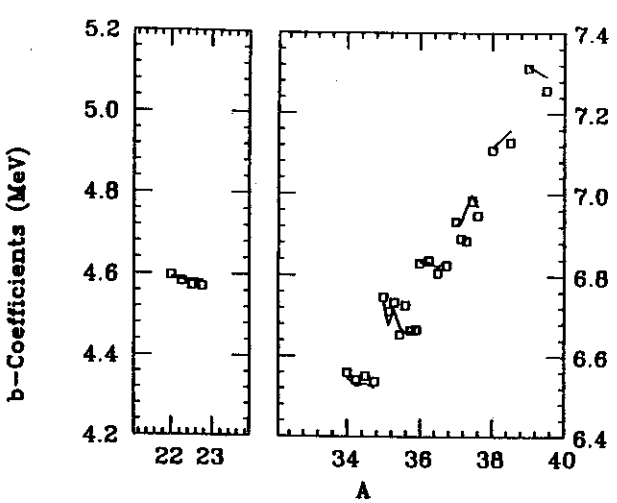


Fig. 2 Plot of 1s-0d-shell b-coefficients. Experimental data are represented by open boxes, while the fitted values are given by the line.

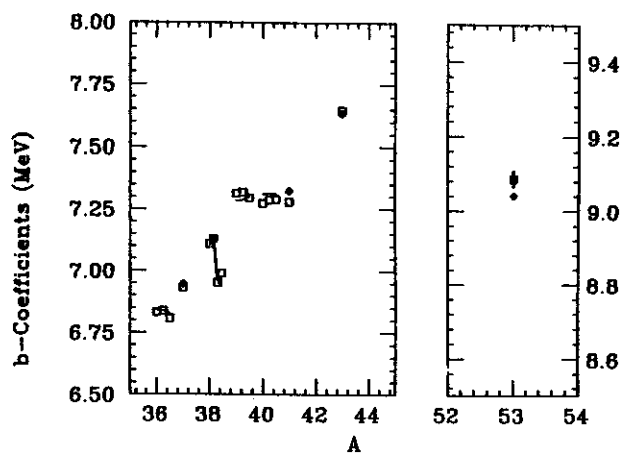


Fig. 3 Plot of $0d_{3/2}$-$0f_{7/2}$-orbit b-coefficients. Experimental data are represented by open boxes, while the fitted values are given by the line and the solid diamonds.

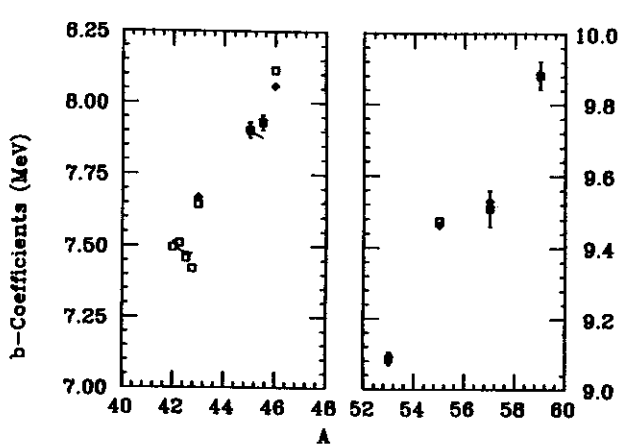


Fig. 4 Plot of 0f-1p-shell b-coefficients. Experimental data are represented by open boxes, while the fitted values are given by the line and the solid diamonds.

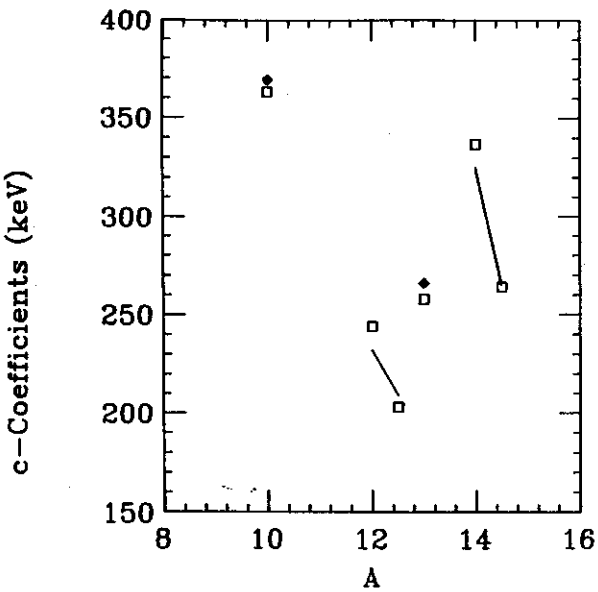


Fig. 5 Plot of 0p-shell c-coefficients. Experimental data are represented by open boxes, while the fitted values are given by the line and the solid diamonds.

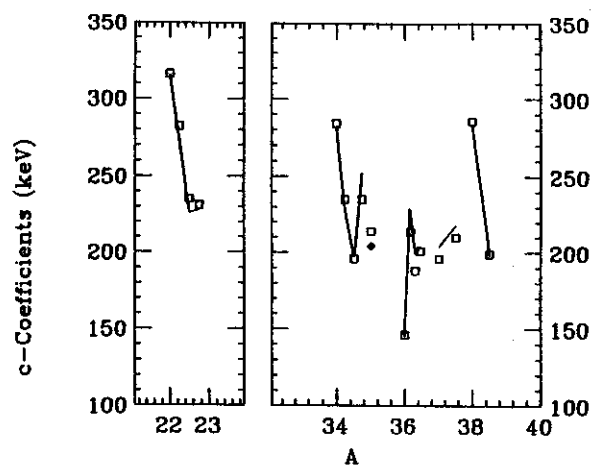


Fig. 6 Plot of 1s-0d-shell c-coefficients. Experimental data are represented by open boxes, while the fitted values are given by the line and the solid diamond.


References

1. E.P. Wigner, Proc. of the Robert A. Welch Conf. on Chem. Research (R.A. Welch Foundation, Houston, Texas, 1957) Vol. 1, p. 67.
2. I.S. Towner and J.C. Hardy, Phys. Lett. 73B (1978)20; J. F. Wilkerson et al., Phys. Rev. Lett. 51(1983)2269; W.E. Ormand and B.A. Brown, submitted to Physics Letters.
3. W.E. Ormand and B.A. Brown, Nucl. Phys. A440(1985)274; W.E. Ormand, Ph.D. thesis, Michigan State University (1985).
4. J.A. Nolen and J.P. Schiffer, Ann. Rev. Nucl. Sci.19(1969).
5. S. Cohen and D. Kurath, Nucl. Phys. 73 (1965)1.
6. B.H. Wildenthal, Progress in Particle and Nuclear Physics, ed. by D.H. Wilkinson (Pergamon Press, Oxford, 1984) Vol. 11, p.5.
7. S.T. Hsieh, R.B.M Mooy, and B.H. Wildenthal, Bull. of American Physical Society 30(1985)731.
8. A.G.M. van Hees and P.W.M. Glaudemans, Zeits. f. Physik A303(1981)267.
9. A.H. Wapstra and K. Bos, 1982 Atomic Mass Evaluation, Nuclear Data Center, Brookhaven National Laboratory (unpublished).
10. F. Ajzenberg-Selove, Nucl. Phys. A375(1982) 1; P.M. Endt and C. Van Der Leun, Nucl. Phys. A310(1978)1; C.M. Lederer and V.S. Shirley, Table of Isotopes, 7th edition (Wiley, New York, 1978).

# THE $(p,\pi^-)$ CONTINUUM

O. Scholten[a] and H. Toki[b]

The continuum spectrum for the $(p,\pi^-)$ reaction at $E_p$=200 to 400 MeV has been calculated in the local Fermi gas model. The absorption of the incoming proton and the outgoing $\pi$ in the nuclear medium are taken into account by using a Glauber theory[1] description. Since the medium corrections on the interaction fields have been found to be important in various phenomena,[2] they are also included in the present work. The detailed formulation is given elsewhere,[3] and only some of the final results are presented here for the calculation of the $(p,\pi^-)$ reaction on $^{42}$Ca, $^{48}$Ca and $^{90}$Zr at 200 MeV. The calculated spectra are compared with experiment[4] in Fig. 1. Although the absolute magnitude of the cross section is overestimated by about a factor two, the structure of the continuum spectrum is well reproduced, as are the relative magnitudes of the cross section for the different targets. The predicted cross section for $^{48}$Ca is about a factor two larger than for $^{42}$Ca, while those for $^{48}$Ca and $^{90}$Zr are about the same. The reason for this lies in a combination of Q-value effects and differences between the proton-neutron distributions at the surface. The fact that the surface is of particular importance in the $(p,\pi^-)$ reaction can be seen from Fig. 2. If the reaction would occur more in the volume part than at the surface, the contribution to the cross section--as a function of impact parameter b--should increase less than linear with b. The reason is that the amount of matter seen by the incoming particle decreases with impact parameter. However, the contribution to the cross section increases more rapidly than linear, to decrease again sharply past the half density radius. The reason for this surface peaking is the strong absorption of both the incoming proton and outgoing pion in the nuclear medium. With increasing energy both of these

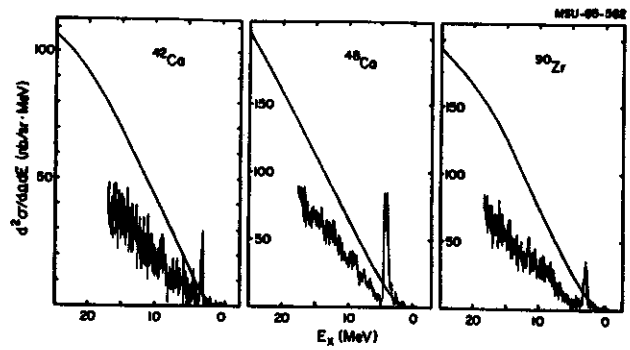


Fig. 1 The calculated continuum cross section at $E_p$=200 MeV as a function of excitation energy is compared with the experimental[4] spectrum measured at $\theta_\pi$=30°.

cross sections increase, resulting in an even stronger surface peaking as shown at 400 MeV in Fig. 2.

The importance of the surface explains part of the ratios of the cross section as observed for the different targets. In $^{48}$Ca the number of neutrons in the surface area is larger than in $^{42}$Ca.[5] Since in the $(p,\pi^-)$ reaction a neutron is converted into a proton, the excess of neutrons explains why the cross section is larger for $^{48}$Ca. In $^{90}$Zr the neutron excess in the surface is smaller, but the surface area has

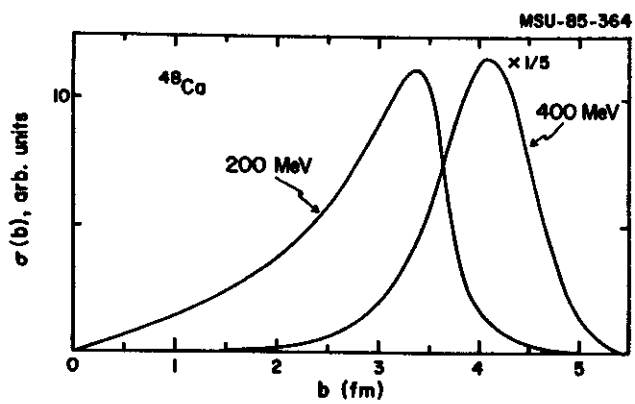


Fig. 2 The contribution to the total cross section for $0<E_x<50$ MeV is plotted as a function of impact parameter at $E_p$=200 MeV and 400 MeV for $^{48}$Ca.

increased. These two counteracting effects give rise to a cross section that is approximately equal to that for $^{48}Ca$. The $(p,\pi^-)$ reaction thus provides a sensitive tool for studying the properties of the nuclear surface.

---

a. On leave: K.V.I., Groningen, The Netherlands
b. Tokyo Metropolitan University, Japan

References

1. R.J. Glauber, Lectures in Theoretical Physics (Interscience, New York) Vol. 1,315 (1959).
2. E. Oset, Y. Futami and H. Toki, Nucl. Phys. (1986) in print.
3. O. Scholten and H. Toki, to be published.
4. S.E. Vigdor et al., Phys. Rev. Lett. 49, 1314(1982); W.W. Jacobs et al., Phys. Rev. Lett. 49,855(1982); S.E. Vigdor et al., Nucl. Phys. A396,61c(1983).
5. J.W. Negele, Phys. Rev. C1,1260 (1974).

# THE OCTUPOLE BOSON INTERACTION IN THE INTERACTING BOSON MODEL

A.F. Barfield[a] and O. Scholten[b]

Negative parity states in even-even nuclei can be described in the Interacting Boson Model (IBM) by coupling the degrees of freedom of a single octupole ($3^-$) motion, called f-boson, to the system of s and d bosons. In analogy with the interaction of an odd-fermion with the system of s, d bosons the interaction for the f-boson is usually written as[1]

$$V_{sdf} = A_2(Q_d^{(2)}\cdot Q_f^{(2)}) + A_3 :(d^\dagger \tilde{f})^{(3)}(f^\dagger \tilde{d})^{(3)}: \quad (1)$$

where for simplicity we have only retained the most important two terms. The quadrupole operators are defined as

$$Q_d^{(2)} = (s^\dagger \tilde{d} + d^\dagger s) + \chi_2 (d^\dagger \tilde{d})^{(2)} \quad (2a)$$

and

$$Q_f^{(2)} = -2\sqrt{7}\ (f^\dagger \tilde{f})^{(2)} \ . \quad (2b)$$

The first term in Eq. (1) arises from the quadrupole interaction of the $3^-$ degree of freedom with the positive parity bosons. The second term is added for purely phenomenological reasons, and is the analog of the "exchange force" in the IBFA model.[2] Without it, it is not possible to obtain a situation where in the negative parity spectrum either a $\kappa=1^-$ or a $\kappa=2^-$ band is lowest. We have investigated the possibility that this component of the force is not related to some exchange mechanism but is related to a neutron-proton octupole interaction.

A neutron-proton octupole interaction, put in boson language, reads

$$V^{oct} = -\kappa_3^{\nu\pi}\, Q_\nu^{(3)}\cdot Q_\pi^{(3)} \quad (3)$$

The octupole operator can in general be written as

$$Q_\tau^{(3)} = (s^\dagger \tilde{f} + f^\dagger s)_\tau^{(3)} + \chi_{3\tau}(d^\dagger \tilde{f} + f^\dagger \tilde{d})_\tau^{(3)} \quad \tau=\nu,\pi \quad (4)$$

In mapping the interaction (3) onto the IBM-1 model space, we make the assumption that the f-boson state of IBM-1 corresponds to the fully symmetric f-boson state of IBM-2. The octupole interaction in IBM-1 now reads

$$V_1^{oct} = -2\,\kappa_3 \frac{N_\nu N_\pi}{N(N-1)} \Big[ (s^\dagger s)(f^\dagger f) - \sqrt{(7/5)}\ ((\chi_{3\nu}\chi_{3\pi})/2)(s^\dagger \tilde{d} + d^\dagger s)\cdot(f^\dagger f)^{(2)} \quad (5)$$

$$-7\ \chi_{3\nu}\chi_{3\pi} \sum_\lambda \sqrt{2\lambda+1} \begin{Bmatrix} 2 & 2 & \lambda \\ 3 & 3 & 3 \end{Bmatrix} ((d^\dagger \tilde{d})^{(\lambda)}(f^\dagger f)^{(\lambda)})^{(0)} \Big]$$

The first term in this expression contributes to the f-boson monopole interaction. The second term contributes to the quadrupole interaction as given in Eq. (1). After some angular momentum recoupling, the third term can be rewritten as

$$3\ \chi_{3\nu}\chi_{3\pi}\kappa_3^{\nu\pi} : (d^\dagger \tilde{f})^{(3)}\cdot(f^\dagger \tilde{d})^{(3)}: \quad (6)$$

with

$$\kappa_3 = -3\kappa^{\nu\pi}\, N_\nu N_\pi / N(N-1) \quad (7)$$

and has precisely the form of the last term in Eq. (1). The relation between the so-called "f-boson exchange" force and the octupole-octupole interaction has thus been established. This also implies a relation between the interaction (1) and the octupole transition operator.[3]

---

a. University of Arizona, Tucson, AZ
b. On leave: K.V.I., Groningen, The Netherlands

## References


1. J. Konijn et al., Nucl. Phys. A352,191 (1981).
2. O. Scholten and A.E.L. Dieperink, Interacting Bose-Fermi Systems in Nuclei, F. Iachello, ed. (Plenum, New York, 1981) p. 285.
3. A.F. Barfield and O. Scholten, to be published.

# THE MASS DEPENDENCE OF EFFECTIVE CHARGES IN IBA

O. Scholten[a] and R.M. Ronningen

The mass dependence of the neutron and proton effective charges in the IBA model has important consequences for the prediction of the E2 transition probability to mixed symmetry states,[1,2] and for the predicted change of the E2 transition strength in a series of isotopes.

There are two distinctly different mechanisms that contribute to the boson effective charge. One of these is core-polarization, the same mechanism that contributes to the shell model effective charges. This mechanism can be assumed to be essentially mass independent (in a limited region). Using shell model effective charges as have been determined for the N=82 isotones,[3] one obtains $e_\nu/e_\pi \sim 0.8/1.8$. The other important contribution comes from truncating the shell model space to the IBM space in which only collective J=0 and J=2 fermion pair states (s and d bosons) are considered. The omission of J=4 collective pairs, hereafter called g-bosons, from the model space especially gives rise to important renormalizations. If it is assumed that the strongest coupling between the s-d boson space and the g-boson sector comes from the neutron-proton quadrupole-quadrupole interaction, this renormalization can be shown to effectively introduce an additional term in the quadrupole operator.[4] Including this additional term, the E2 transition operator can be written as

$$\tilde{T}^{(E2)} = \bar{e}_\nu Q_\nu^{(2)} + \bar{e}_\pi Q_\pi^{(2)} + \alpha_\pi \bar{e}_\pi \hat{n}_{d_\pi} Q_\nu^{(2)} + \alpha_\nu \bar{e}_\nu \hat{n}_{d_\nu} Q_\pi^{(2)} \quad (1)$$

where $\bar{e}$ are the bare boson charges. The coefficients $\alpha$ are proportional to the interaction strength between the g-boson and the s-d boson space. Taking for simplicity $\alpha_\nu = \alpha_\pi = \alpha$, the (s-d) boson effective charges can be written as

$$e_\nu = \bar{e}_\nu + \alpha \bar{e}_\pi \langle \hat{n}_{d_\pi} Q_\nu^{(2)} \rangle / \langle Q_\nu^{(2)} \rangle ,$$
$$e_\pi = \bar{e}_\pi + \alpha \bar{e}_\nu \langle \hat{n}_{d_\nu} Q_\pi^{(2)} \rangle / \langle Q_\pi^{(2)} \rangle \quad (2)$$

where the brackets <> denote expectation values. In Table 1 these are tabulated for the Nd isotopes, for the $2_1^+ \rightarrow 0_1^+$ transitions. Taking $\bar{e}_\pi/\bar{e}_\nu = 2.25$ as discussed above for the ratio of bare charges, $\alpha = 0.8$, and $\bar{e}_\pi = 0.104$ eb, we now obtain the (s-d) bosons effective charges, e, and $(2_1^+ \rightarrow 0_1^+)$ matrix elements as given in Table 1 where they are compared with experiment.

As is discussed in Refs. 4 and 5 the g-boson renormalizations also strongly affect the single d-boson energies, $\varepsilon$. By using the

Table 1. Expectation values of the operators necessary to calculate the boson effective charges for the $2_1^+ \rightarrow 0_1^+$ transitions in Nd are given. In addition, the deduced effective charges and calculated transition matrix elements are given, using the parameters discussed in the text. The experimental values of M(E2), the absolute values of the square-roots of B(E2), are given in the last column along with that for $^{142}$Nd (Refs. 6 and 7).

| A | $\langle Q_\nu \rangle$ | $\langle \hat{n}_{d_\pi} Q_\nu \rangle$ | $\langle Q_\pi \rangle$ | $\langle \hat{n}_{d_\nu} Q_\pi \rangle$ | $e_\nu$[eb] | $e_\pi$[eb] | $M(E2;2_1^+ \rightarrow 0_1^+)$[eb] Calc | Exp |
|---|---|---|---|---|---|---|---|---|
| 142 | 0.0 | 0.0 | 5.0 | 0.0 | ----- | 0.104 | 0.52 | 0.53(4) |
| 144 | 1.39 | 0.38 | 4.97 | 1.15 | 0.069 | 0.113 | 0.66 | 0.76(1) |
| 146 | 2.54 | 1.45 | 5.22 | 2.68 | 0.094 | 0.123 | 0.88 | 0.88(1) |
| 148 | 3.80 | 2.83 | 5.19 | 3.92 | 0.108 | 0.132 | 1.09 | 1.178(9) |
| 150 | 5.37 | 6.21 | 5.84 | 7.49 | 0.143 | 0.152 | 1.66 | 1.678(11) |

formulas given in Ref. 4 an order-of-magnitude estimate of the parameter $\alpha$ can be made from the reduction of $\varepsilon$ as compared to its value in semiclosed shell nuclei,

$$\alpha_\pi \simeq \frac{\varepsilon_0 - \varepsilon}{5 N_\nu k} , \qquad (3)$$

where $\varepsilon_0$ is the energy of the $2^+$ state in the semiclosed shell nucleus and $N_\nu$ the number of neutron bosons. Using the parameter values deduced for Nd and $\varepsilon_0$=1.6 MeV, values for $\alpha$ of the order of 0.6 are obtained, which are in excellent agreement with the value of 0.8 used in the present calculation.

---

a. Present address: K.V.I., Groningen, The Netherlands

References

1. W.D. Hamilton et al., Phys. Rev. Lett. 53,2469(1984).
2. T. Otsuka and J.N. Ginocchio, Phys. Rev. Lett. 54,777(1985).
3. O. Scholten and H. Kruse, Phys. Lett. 125B, 113(1983).
4. O. Scholten, Phys. Lett. 119B,5(1982).
5. T. Otsuka, Nucl. Phys. A368,244(1981).
6. P.M. Endt, At. Data and Nucl. Data Tables 26,48(1981).
7. A.Y. Ahmed et al., to be published.

# COMPARISONS OF IBFA AND TRIAXIAL CALCULATIONS FOR ODD-MASS N=80 NUCLEI

R. Aryaeinejad and Wm.C. McHarris

The two most important models to describe and interpret excited states in odd-mass N=80 isotones are the triaxial weak-coupling model[1] and interacting boson-fermion model[2]. We have previously performed the triaxial calculations for $^{143}$Eu, $^{141}$Pm and $^{139}$Pr nuclei [3-5] which predict an oblate shape for all of them. Although this model seems to do a fairly good job of describing the levels structure of these nuclei at low excitation energy, the results are less satisfactory for high excited states.

So far the interacting boson-fermion model has been applied to a few odd-mass nuclei. More recent systematic studies of Eu and Pm isotopes[6,7] proved that this model is very successfull in describing the level structure of these nuclei ranging from spherical to deformed shape. The main motivations for the present investigation are, first to compare this model with the triaxial model, second to extend the systematics to the region below N=82 in combination with previous calculations of Eu and Pm isotopes above N=82.

To describe the N=80 isotones the odd proton is coupled to a core with the same number of neutrons. The parameters describing the cores have been obtained from a IBA-1 calculations for the $^{142}$Sm, $^{140}$Nd and $^{138}$Ce nuclei. These are given in Table I.

Table I. core parameters used in IBA-1.

| CORE | $\varepsilon$ | $\kappa$ | $\kappa'$ | $\chi$ |
|---|---|---|---|---|
| $^{142}$Sm | .90 | -.04 | .03 | 2.5 |
| $^{140}$Nd | .75 | -.015 | .028 | 2.26 |
| $^{130}$Ce | .77 | -.015 | .02 | 2.26 |

The negative parity levels are built on the $h_{11/2}$ single particle orbit. The positive parity levels, are generated by coupling $d_{5/2}$ and $g_{9/2}$ orbits to the core. The $d_{3/2}$ and $s_{1/2}$ orbitals can be neglected due to the energy gap in the single particle energies (the effect is negligible on the low lying states). In the IBFA calculations the parameters were adjusted for each isotope separately so as to give a good overall fit to the experimental excitation energies while insisting that parameters varied smoothly and systematically as a function of z. These parameters are listed in Table II.

Table II. parameters used in IBFA calculations.

| ORBIT | NUCLEUS | $a_j$ | $\chi$ | $v_j^2$ | $\Gamma_o$ | $\Lambda_o$ |
|---|---|---|---|---|---|---|
| $h_{11/2}$ | $^{143}$Eu | -.2 | .36 | .2 | .56 | 1.7 |
| | $^{141}$Pm | -.2 | .70 | .2 | .56 | 1.7 |
| | $^{139}$Pr | -.5 | .70 | .1 | .56 | 2.2 |
| $d_{5/2}$ | $^{143}$Eu | -.2 | .36 | .70,.8 | .56 | 1.88 |
| $g_{7/2}$ | $^{141}$Pm | -.2 | .70 | .75,.8 | .56 | 1.4 |
| | $^{139}$Pr | -.1 | .70 | .75,.8 | .56 | 1.8 |

The results of calculated excitation energies are compared with experiment and those of a triaxial calculations in Fig. 1 for negative parity states and in Fig. 2 for positive parity states. All spectra show more or less the characteristic of a particle vibrational spectrum ( SU(5) symmetry ), with the lowest lying $5/2^+$, $7/2^+$ and $11/2^-$ levels being the single particle states.

For negative parity states, the experimental energy levels are reproduced very well in the IBFA calculations, although it is difficult to make a correlations due to uncertain spin assignments. In the triaxial

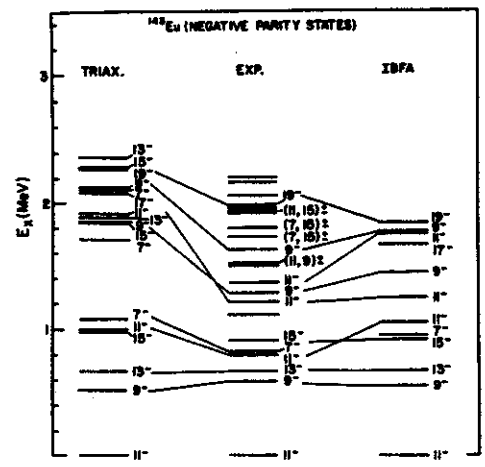


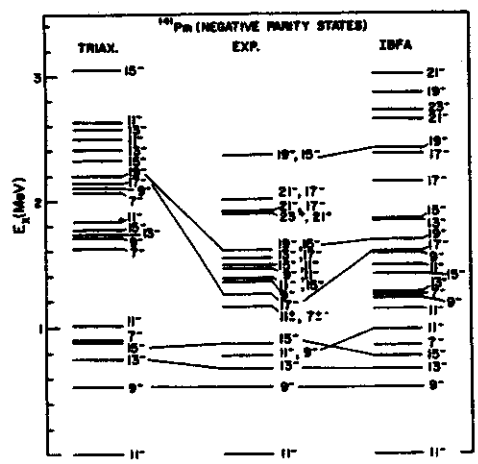


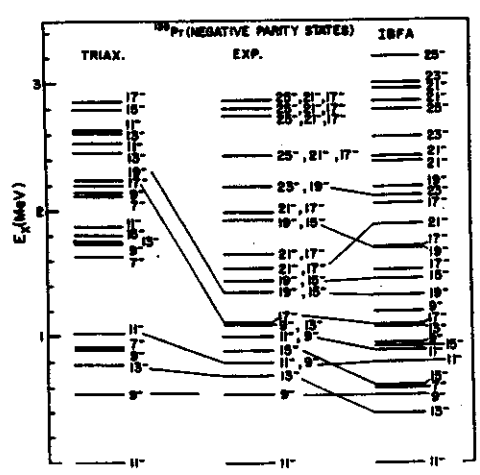


Fig. 2 Experimental and calculated positive parity levels of the odd-mass N=80 isotones. The spins are shown in 2J.

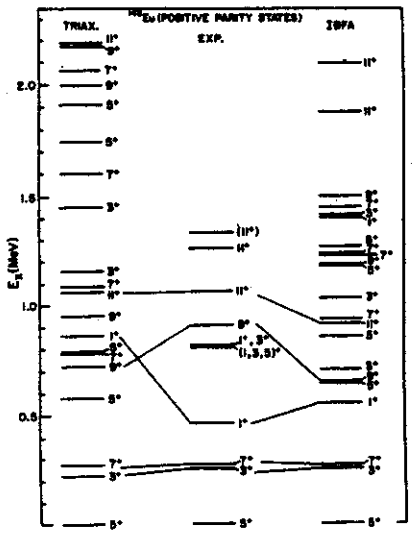


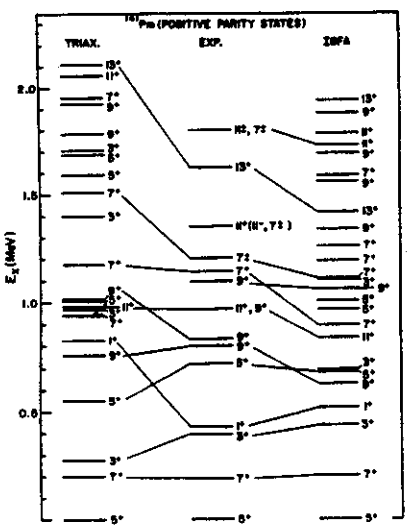


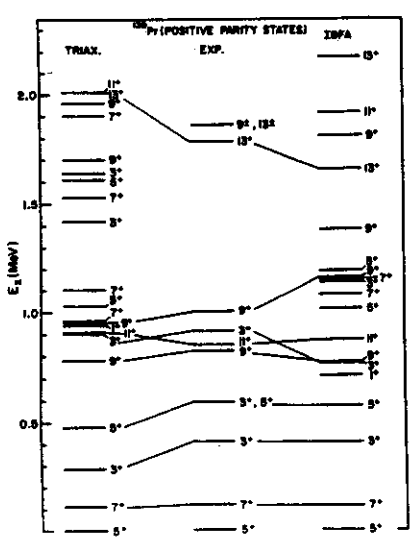


Fig. 1 Experimental and calculated negative parity levels of the odd-mass N=80 isotones. The spins are shown in 2J.

calculations however, the predicted levels of high lying states are too high compared to the experiment and to IBFA calculations. This is because a pure quadrupole coupling of triaxial model is insufficient to reproduce the experimental data. On the other hand, the IBFA calculations, which include the exchange force between fermion and core, give much better agreement with the experiment. In the case of positive parity states (Fig. 2), both models seem to be giving (with few exceptions) the same results up to about 1 MeV in excitation energy. One of the exceptions is $J^{\pi}=1/2^{+}$ in $^{143}$Eu and $^{141}$Pm which is predicted too high in the triaxial model. It is evident that above 1 MeV, the triaxial calculations are no longer in agreement with the experiment.

Detailed calculations of spectroscopic factors and transition rates for these isotones are in progress in order to further distinguish between these two models.

---

References


1. J. Meyer-ter-Vehn, Nucl. Phys. A249, 111(1975).
2. F. Iachello and O. Scholten Phys. Rev. Lett. 43,679(1979).
3. R. Aryaeinejad et al. Phys. Rev. C.23,194(1981).
4. R. Aryaeinejad et al. Phys. Rev. C. 32,1855(1985).
5. R. Aryaeinejad and Wm.C. McHarris, to be published.
6. O. Scholten and N. Blasi, Nucl. Phys. A380,509(1982).
7. O. Scholten T. Ozzello, Nucl. Phys. A424,221(1984)